

Studies in Surface Science and Catalysis 12

# METAL MICROSTRUCTURES IN ZEOLITES

Preparation – Properties – Applications

Proceedings of a Workshop, Bremen, September 22–24, 1982

Editors

**P.A. Jacobs**

*Centrum voor Oppervlaktescheikunde, Katholieke Universiteit Leuven, Leuven, Belgium*

**N.I. Jaeger**

*Forschungsgruppe Angewandte Katalyse, Universität Bremen, Bremen, F.R.G.*

**P. Jirů**

*Czechoslovak Academy of Sciences, J. Heyrovský Institute of Physical Chemistry and Electrochemistry, Prague, Czechoslovakia*

**G. Schulz-Ekloff**

*Forschungsgruppe Angewandte Katalyse, Universität Bremen, Bremen, F.R.G.*



ELSEVIER SCIENTIFIC PUBLISHING COMPANY

Amsterdam – Oxford – New York

1982

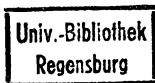
84/19138

86/VE, 7048, J12

ELSEVIER SCIENTIFIC PUBLISHING COMPANY  
Molenwerf 1  
P.O. Box 211, 1000 AE Amsterdam, The Netherlands

*Distributors for the United States and Canada:*

ELSEVIER SCIENCE PUBLISHING COMPANY INC.  
52, Vanderbilt Avenue  
New York, NY 10017



7 068 520

**Library of Congress Cataloging in Publication Data**  
Main entry under title:

Metal microstructures in zeolites.

(Studies in surface science and catalysis ; v. 12)  
Sponsored by Deutsche Forschungsgemeinschaft, and  
others.

Includes index.

1. Zeolites--Congresses. 2. Microstructure--Congresses.  
es. I. Jacobs, Peter A. II. Deutsche Forschungsgemein-  
schaft (1951- ) III. Series.  
TP159.M6M47 1982 666'.86 82-13732  
ISBN 0-444-42112-2 (U.S.)

ISBN 0-444-42112-2 (Vol. 12)  
ISBN 0-444-41801-6 (Series)

© Elsevier Scientific Publishing Company, 1982

All rights reserved. No part of this publication may be reproduced, stored in a retrieval system or transmitted in any form or by any means, electronic, mechanical, photocopying, recording or otherwise, without the prior written permission of the publisher, Elsevier Scientific Publishing Company, P.O. Box 330, 1000 AH Amsterdam, The Netherlands

Printed in The Netherlands

## CONTENTS

Preface	VII
The chemistry of ruthenium in zeolites (J.H. Lunsford)	1
EPR studies of Co(II)-bis(dimethylglyoximato)-complexes and their oxygen adducts in a zeolite X matrix C.J. Winscom, W. Lubitz, H. Diegruber and R. Möselner)	15
In-situ-UV/VIS-microsopespectrophotometry of reactions of $\text{Co}^{2+}$ -complexes within single crystals of faujasite-type zeolites (H. Diegruber and P.J. Plath)	23
Mossbauer spectroscopic studies of ferrous ion exchange in zeolite A (L.V.C. Rees)	33
Metal inclusion complexes of zeolite A (N. Petranović and R. Dimitrijević)	45
Quantum chemical study of the properties of Fe, Co, Ni and Cr ion-exchanged zeolites (S. Beran and P. Jirů)	53
Cationic rhodium complexes and rhodium metal aggregates in zeolite Y (H. van Brabant, R.A. Schoonheydt and J. Pelgrims)	61
Mechanisms of formation and stabilization of metals in the pore structure of zeolites (P.A. Jacobs)	71
Reflectance spectroscopic study of $\text{Ag}^+$ , $\text{Ag}^0$ and Ag clusters in zeolites of the faujasite-type (L.R. Gellens and R.A. Schoonheydt)	87
Chemical evidence for charged clusters in silver zeolites (H.K. Beyer and P.A. Jacobs)	95
UV/VIS transmission spectroscopy of silver zeolites. I. Dehydration and rehydration of AgA and AgX (H.G. Karge)	103
Adsorption and decomposition of iron pentacarbonyl on Y zeolites (Th. Bein, P.A. Jacobs and F. Schmidt)	111
Stabilization and characterization of metal aggregates in zeolites. Catalytic properties in $\text{CO} + \text{H}_2$ conversion (D. Ballivet-Tkatchenko, G. Coudurier and Nguyễn Duc Chau)	123
Influence of controlled structural changes on the catalytic properties of zeolites (P. Jirů)	137
Behaviour of Fe species in zeolite structure (B. Wichterlová, L. Kubelková, J. Nováková and P. Jirů)	143
To the differences in properties of Ni metal particles and Cr cations in stabilized and nonstabilized zeolites (V. Patzelová, Z. Tvarůžková, K. Mach and A. Zúkal)	151

## VI

Incorporation of volatile metal compounds into zeolitic frameworks (P. Fejes, I. Kiricsi and I. Hannus)	159
Characterization of metal aggregates in zeolites (P. Gallezot and G. Bergeret)	167
Nuclear magnetic resonance study of xenon adsorbed on metal-NaY zeolites (size of metal particles and chemisorption) (J. Fraissard, T. Ito, L.C. de Menorval and M.A. Springuel-Huet)	179
Characterization of metal aggregates in zeolites (F. Schmidt)	191
Electron microscopical analysis of monodispersed Ni and Pd in a faujasite X matrix (D. Exner, N.I. Jaeger, K. Möller, R. Nowak, H. Schrübbers, G. Schulz-Ekloff and P. Ryder)	205
Investigations of the aggregation state of metals in zeolites by magnetic methods (W. Romanowski)	213
Dielectric properties of X-type zeolites containing small metallic nickel particles (J.C. Carru and D. Delafosse)	221
Modification of chemisorptive and catalytic properties of Ni <sup>0</sup> highly dispersed on zeolites of various composition (G.N. Sauvion, M.F. Guilleux, J.F. Tempere and D. Delafosse)	229
Nickel in mordenites - formation and activity of metallic complexes, clusters and particles (E.D. Garbowski, C. Mirodatos and M. Primet)	235
Dispersion of nickel and ruthenium in zeolites L, Y and mordenite (S. Narayanan)	245
Effect of the reaction medium on the metal microstructure of nickel-zeolite catalysts (N.P. Davidova, M.L. Valcheva and D.M. Shopov)	253
Activities and selectivities of reduced NiCaX faujasites in the carbon monoxide hydrogenation reaction (H. Schrübbers, G. Schulz-Ekloff and G. Wildeboer)	261
Fischer-Tropsch synthesis on polyfunctional manganese/iron-pentasil zeolite catalysts (K. Müller, W.-D. Deckwer and M. Ralek)	267
Oxidation of ethylene on silver-loaded natural zeolites (G. Bagnasco, P. Ciambelli, E. Czarán, J. Papp and G. Russo)	275
Author Index	283

## ADSORPTION AND DECOMPOSITION OF IRON PENTACARBONYL ON Y ZEOLITES

Th. BEIN<sup>1,3</sup>, P.A. JACOBS<sup>2</sup> and F. SCHMIDT<sup>1</sup><sup>1</sup>Institut für Physikalische Chemie der Universität Hamburg, Laufgraben 24,  
D-2000 Hamburg 13 (F.R.G.)<sup>2</sup>Centrum voor Oppervlaktescheikunde en Colloïdale Scheikunde, Katholieke  
Universiteit Leuven, De Croylaan 42, B-3030 Leuven (Heverlee) (Belgium)<sup>3</sup>Present address : 2

## ABSTRACT

The adsorption isotherms of  $\text{Fe}(\text{CO})_5$  on NaY and HY zeolites obtained in McBain balances show micropore adsorption, the saturation at  $p/p_0 = 0.5$  being 39 and 42 % per dry wt, respectively. IR results indicate a restricted mobility of the engaged complex. Nevertheless it can thermally be desorbed to a great extent in vacuum.

For the first time, well distinguishable decomposition phases of zeolite-adsorbed  $\text{Fe}(\text{CO})_5$  are found by thermogravimetric analysis. These phases are associated with species bearing 2(4) and 1/4(1) CO ligands per Fe in the case of NaY(HY). New evidence is found for the intermediate  $\text{Fe}_3(\text{CO})_{12}$ . The slow decomposition reaction in inert atmosphere is completed already between 70 and 90°C, providing an iron content of  $10.5 \pm 0.5$  wt %.

## INTRODUCTION

With respect to the industrial importance of iron catalysts and the still not entirely understood particle size effect in catalysis, it is desirable to dispose of model catalysts with variable, narrow particle size distribution. Zeolites have proved to be suitable supports for metals (ref. 1,2) and to behave as model catalysts. Our aim is therefore to obtain Fe(0) containing zeolites with narrow particle size distributions. Reduction of Fe(II) exchanged Y-type zeolites was found to be impossible with  $\text{H}_2$  (ref. 3,4), whereas reduction with sodium vapor resulted in highly dispersed iron metal (ref. 5-8).

With regard to the difficult procedures to be used in these methods, the decomposition of Y-zeolite adsorbed iron pentacarbonyl was chosen as an alternative.

Thermal decomposition of this complex has already been used to prepare dispersed supported iron (ref. 9), while recently it has been applied to  $\text{Fe}(\text{CO})_5$  loaded HY zeolite (ref. 10-12). In addition, decomposition by UV light was reported to provide a highly dispersed iron phase in the HY zeolite.

In the former studies, few quantitative details are given with regard to the parameters which govern adsorption and decomposition of the complex. In order

to arrive at a quantitative understanding of these processes, the adsorption and decomposition behaviour of iron pentacarbonyl in NaY and HY zeolite has been studied by means of gravimetric, thermogravimetric and IR-spectroscopic methods.

## EXPERIMENTAL

### Materials

Synthetic NaY with Si/Al = 2.46 was from Strem Chemicals. It was treated with 0.1 M NaCl solution to remove possible cation deficiencies, washed and air dried, and stored over saturated  $\text{NH}_4\text{Cl}$  solution. The  $\text{NH}_4\text{Y}$  form was obtained by conventional ion exchange. Before loading with iron carbonyl, both zeolites were degassed in situ at  $450^\circ\text{C}$  for about 12 hrs at  $10^{-5}$  mbar, at a heating rate of  $2^\circ\text{C}/\text{min}$ .

Iron pentacarbonyl from Ventron (99.5 %) was cold distilled in the dark and stored over molecular sieve 5A. The zeolite samples for the McBain and IR measurements were loaded with the carbonyl as follows. The frozen carbonyl was outgassed in vacuum and allowed to warm up until the desired pressure was reached. All procedures with  $\text{Fe}(\text{CO})_5$  were performed in the dark, whereas the weight measurements at the McBain balance have been carried out in weak red light.

### Methods

Adsorption isotherms were obtained in a McBain balance with calibrated quartz spring, with a precision of  $\pm 0.5\%$ . The pressure was measured with a Bell & Howell pressure transducer BHL-4100-01, which is linear within  $\pm 0.5\%$  up to 750 mbar.

Infrared spectra were taken with a Perkin Elmer 580B spectrometer from 4000 to  $1200\text{ cm}^{-1}$  (resolution  $2\text{ cm}^{-1}$ ) using a quartz cell with 80 mm path length and equipped with CaF windows of 3 mm thickness. The zeolite was pressed at  $1\text{ ton}/\text{cm}^2$  to selfsupporting films of ca.  $5\text{ mg}/\text{cm}^2$ . All treatments were performed in situ in the IR cell.

Thermogravimetric measurements were done on a Mettler Thermoanalyzer 2 under He purge, mostly in the 10 mg range. Samples of 5 to 50 mg zeolite were outgassed by heating at  $2^\circ\text{C}/\text{min}$  up to  $450^\circ$  in a quartz oven and loaded at  $20^\circ\text{C}$  in a stream of dry helium containing ca. 4 mbar  $\text{Fe}(\text{CO})_5$ . The flow rate of this stream was 2.8 l/h.

## RESULTS AND DISCUSSION

### 1. Adsorption isotherms of $\text{Fe}(\text{CO})_5$ on Y-zeolite

Comparison of the  $\text{Fe}(\text{CO})_5$  adsorption isotherms on NaY and HY shows rather similar behaviour (Fig. 1). The major uptake occurs at very low partial

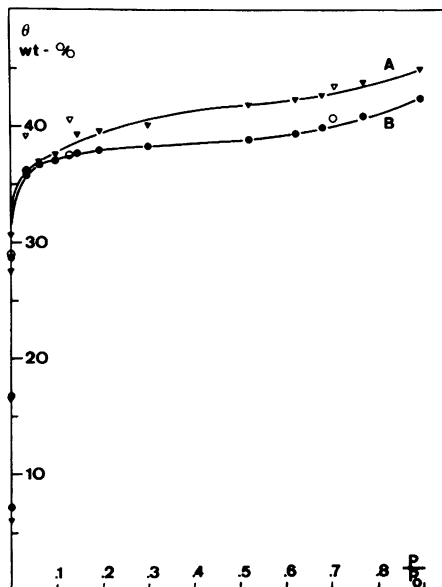


Fig. 1. Adsorption isotherms of  $\text{Fe}(\text{CO})_5$  on (A) HY- and (B) NaY-zeolite at  $20^\circ\text{C}$  [ $p_0 = 29.4$  mbar]. Full points : adsorption; open points : desorption.

pressures and remains almost constant up to  $p/p_0 \approx 0.5$ . At this partial pressure NaY and HY adsorb 39 and 42 mg of  $\text{Fe}(\text{CO})_5$  per 100 mg of dry zeolite, respectively.

Desorption is reversible down to ca.  $p/p_0 = 0.1$ . After degassing for 15 hrs at  $10^{-5}$  mbar,  $\text{Fe}(\text{CO})_5$  loadings of 29 and 27 wt % are obtained for NaY and HY, respectively.

The adsorption behaviour can be explained in terms of nearly ideal micropore adsorption (ref. 13), the micropores being the supercages of the faujasite. The amount  $\text{Fe}(\text{CO})_5$  adsorbed before capillary condensation occurs corresponds to 25 molecules/U.C. or 3.1 molecules per supercage. If an effective radius of 0.30 nm is assumed for the complex, the geometry of the supercages allows a maximum adsorption of three molecules per supercage.

This good agreement with the experimental results confirms the picture of completely filled supercages.

## 2. Infrared study of $\text{Fe}(\text{CO})_5$ adsorbed on zeolite Y

The  $\text{Fe}(\text{CO})_5$  saturated zeolite wafers show no measurable transmission in the CO-stretching region. The IR spectra reported in Fig. 2 correspond therefore to samples loaded with about 10 % of the capacity obtained at saturation. The carbonyl vibrations show a rather similar pattern for both NaY and HY,

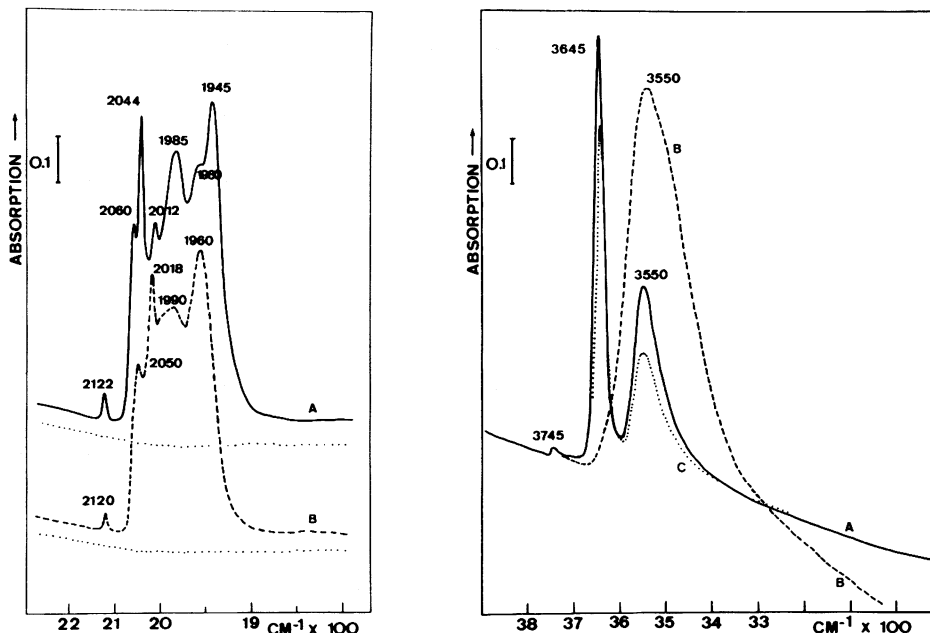


Fig. 2. (left) IR spectra of  $\text{Fe}(\text{CO})_5$ /zeolite adducts at  $20^\circ\text{C}$  (saturated for 10 %). A :  $\text{Fe}(\text{CO})_5/\text{NaY}$ ; B :  $\text{Fe}(\text{CO})_5/\text{HY}$ ; dotted lines : zeolites degassed at  $450^\circ\text{C}$ .

Fig. 3. (right) OH spectrum of saturated  $\text{Fe}(\text{CO})_5/\text{HY}$  adduct decomposed in 600 mbar He. A : zeolite degassed at  $450^\circ\text{C}$ ; B : HY saturated with  $\text{Fe}(\text{CO})_5$  at  $20^\circ\text{C}$ ; C : sample B after heating at  $150^\circ\text{C}$  for 45 min.

respectively (Table 1<sup>a</sup>). Compared to the HY-adduct,  $\text{Fe}(\text{CO})_5$  adsorbed on NaY exhibits two additional bands at  $2044$  and  $1945\text{ cm}^{-1}$ , all other bands only slightly being changed.

The carbonyl bands cannot be assigned definitely to particular species inside the zeolite cages. The assignment of the carbonyl bands to monosubstituted species as  $\text{ZOH}\text{---Fe}(\text{CO})_4$  (ref. 11,12) seems to be somewhat arbitrary because of the fortuitous agreement of some bands with those of complexes such as  $\text{Fe}(\text{CO})_4\text{P}(\text{CH}_3)_3$ .

By  $^{13}\text{C}$ -nmr line-width broadening, a restricted mobility of the  $\text{Fe}(\text{CO})_5$  adsorbed in HY was found (10). This is quite reasonable since the adsorption experiments indicate complete filling of the supercages. The carbonyl bands of crystalline  $\text{Fe}(\text{CO})_5$  and of the  $\text{Fe}(\text{CO})_5$ /zeolite adducts (Table 1) show fairly good agreement, although the intensities are different. This also is in line with the restricted mobility of the complex in the supercages.

In particular, the appearance of the sharp  $2122\text{ cm}^{-1}$  band can be explained by decreased site symmetry. Indeed, the intensity of the  $\nu_1$  mode increases on



TABLE 1

IR frequencies of  $\text{Fe}(\text{CO})_5$  and its adducts (CO-stretching region).

Adduct	Frequency/ $\text{cm}^{-1}$						Ref.
$\text{Fe}(\text{CO})_5/\text{NaY}$	2122w	2060s	2044s	2012s	1985s	1960sh 1945s	a
$\text{Fe}(\text{CO})_5/\text{HY}$	2120w	2050s		2018s	1990b	1960s	a
$\text{Fe}(\text{CO})_5/\text{HY}$	2112mw	2040s	2030sh	2010s	1985sh	1950ms	12
$\text{Fe}(\text{CO})_5$ solid $\bar{5}$ (-173°C)	2115( $\nu_1$ )	2033( $\nu_2$ )	2017sh	2003( $\nu_6$ )	1980( $\nu_{10}$ )	1956/48( $^{13}\text{C}$ )	14
$\text{Fe}(\text{CO})_5$ liquid $\bar{5}$ (25°C)		[broad]		2002( $\nu_6$ )	1979( $\nu_{10}$ )		15
$\text{Fe}(\text{CO})_5$ gas (25°C)			2034vvs( $\nu_6^4$ )		2014vvs( $\nu_{10}$ )		16

<sup>a</sup>This work.

going from the gas phase to crystalline state (ref. 14).

The IR spectrum of liquid  $\text{Fe}(\text{CO})_5$  exhibits a broad and poorly structured CO stretching band around  $2000 \text{ cm}^{-1}$  (Table 1). This also is in contrast to the observed well structured CO-bands of the  $\text{Fe}(\text{CO})_5/\text{zeolite}$  adducts.

In both the NaY and the HY adduct no  $\nu_{\text{CO}}$ -bridging are shown, i.e., at 20°C no clusters with bridging CO ligands such as  $\text{Fe}_2(\text{CO})_9$  are generated.

The interaction of  $\text{Fe}(\text{CO})_5$  with the OH-bands of HY is illustrated in Fig. 3. Only the supercage hydroxyl groups ( $3645 \text{ cm}^{-1}$ ) disappear completely upon adsorption of the carbonyl. The band at  $3550 \text{ cm}^{-1}$  broadens and increases in intensity. This can only be explained by the formation of an hydrogen bond of moderate strength between the complex and the supercage OH-groups.

### 3. Desorption of $\text{Fe}(\text{CO})_5$ from Y zeolite

Heating the  $\text{Fe}(\text{CO})_5$  loaded zeolite wafers in a vacuum of  $10^{-4}$  mbar results in a proportional decrease of intensity of all carbonyl bands, while no new bands appear (Fig. 4).

When the similar experiments are carried out on larger amounts of sample (100 mg), iron losses between 20 and 50 % with respect to carbonyl saturation are determined gravimetrically.

These observations must be explained by desorption of the iron complex, which also may be the reason for the different iron loadings obtained by other authors (ref. 10-12) after thermal decomposition in vacuum, with values ranging from 1 to 8 wt % Fe. The proportional decrease of all carbonyl bands (Fig. 4) also indicates that one single species is adsorbed in the zeolite cage, which seems to be the intact  $\text{Fe}(\text{CO})_5$ .

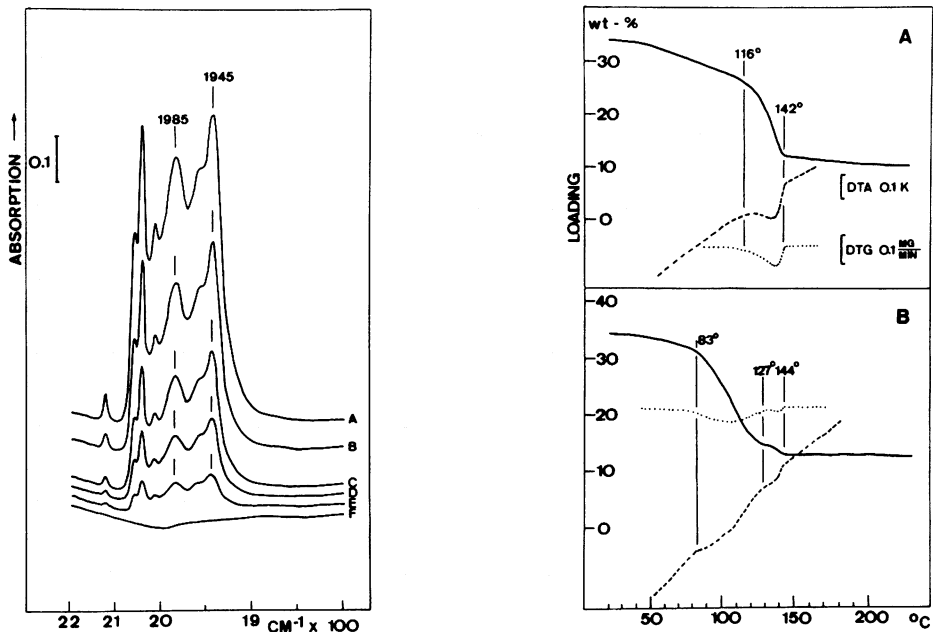


Fig. 4. (left) IR spectra of the desorption process of the 10 % saturated  $\text{Fe}(\text{CO})_5/\text{Na}$  adduct upon heating in vacuum. A : initial loading at  $20^\circ\text{C}$ ; B : heating at  $40^\circ\text{C}$  for 45 min; C : at  $60^\circ\text{C}$  for 30 min; D : at  $65^\circ\text{C}$  for 20 min; E : at  $65^\circ\text{C}$  for 40 min; F : at  $65^\circ\text{C}$  for 100 min.

Fig. 5. (right) Thermogramm of the decarbonylation of  $\text{Fe}(\text{CO})_5/\text{zeolite}$  adducts in He flow. (Heating rate :  $1^\circ\text{C}/\text{min}$  to  $200^\circ\text{C}$ ). A :  $\text{Fe}(\text{CO})_5/\text{NaY}$  (saturated), 8.90 mg dry wt; B :  $\text{Fe}(\text{CO})_5/\text{HY}$  (saturated, 9.65 mg dry wt. Full line = TG curve; dashed line = DTA; dotted line = DTG.

#### 4. Decarbonylation of $\text{Fe}(\text{CO})_5/\text{zeolite}$ adducts by thermoanalysis

When in a thermobalance different amounts of zeolite are loaded with carbonyl vapor, the saturation loadings correspond to the adsorption isotherms (38 wt %). Samples are heated up to  $200^\circ\text{C}$  in a He stream at rates from 0.2 to  $2^\circ\text{C}/\text{min}$ .

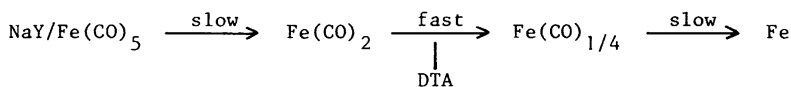
a. Decomposition of  $\text{Fe}(\text{CO})_5/\text{NaY}$ . Irrespective of the amount of sample and the heating rate, three distinct regions are found with respect to thermal behaviour. Two zones of slow weight loss are separated by a fast decrease in sample weight (Fig. 5A). The latter is accompanied by an endothermic DTA effect. It is striking, that the DTA effect always starts, when the sample has lost 15 wt % of its loading. The begin of the third zone is defined by the end of the DTA effect and always occurs when 26 wt % of loading are lost. Around  $200^\circ\text{C}$ , the sample weight becomes stable and corresponds to a loading of 10.5 %.

Begin- and end-temperature of the DTA effect are strongly dependent on the

heating rate. Extrapolation of these temperatures to zero heating rate (ref. 17) indicates, that the same decomposition can be performed isothermally in the temperature region between 70 and 90°C. An isothermal experiment at 90°C after 11 hrs showed the break in the weight curve. Since the sample weight does not change from 200 to 400°C, the adsorbate present is considered to be metallic iron. Compared to the original carbonyl loading losses of iron must be smaller than 0.5 wt %.

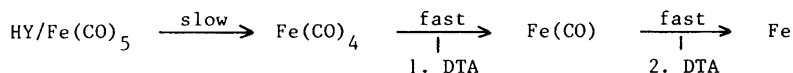
This is in contrast to the results of vacuum decomposition and can be explained by an efficient hindering of the carbonyl diffusion at high pressures of inert gas.

The thermoanalytical results allow to depict carbonyl decomposition on NaY as follows :



The agreement between the measured weight loss and the one calculated according to this stoichiometry lies within 5 %.

b. Decomposition of Fe(CO)<sub>5</sub>/HY. The thermogramm of the HY/Fe(CO)<sub>5</sub> adduct is distinctly different from the one of the NaY adduct (Fig. 5B). First, the fast decomposition as indicated by the start of the DTA effect always appears at lower temperatures (83°C). Second, two weak, but reproducible endotherm DTA effects are observed instead of one, which correlate with the DTG minima. Above 144°C (the endpoint of the second DTA effect) no further weight loss occurs. Similar considerations as with NaY lead to the following stages of decomposition :



Again, excellent agreement between calculated and measured values is obtained.

In previous work decomposition of Fe(CO)<sub>5</sub>/HY in vacuum was reported to start at 25°C and to be complete at 200°C (ref. 12). The formation of Fe(CO)/HY is postulated in vacuo at 70°C (ref. 10). In these studies no reaction times were reported.

From our results it is clear that the temperature for complete decomposition is below 90°C and that decomposition is a very slow reaction.

### 5. In situ investigation of the $\text{Fe}(\text{CO})_5$ /zeolite decomposition by IR spectroscopy

Decomposition of the carbonyl adducts in a He atmosphere leads to results quite distinct from those of vacuum heating. For the  $\text{Fe}(\text{CO})_5/\text{NaY}$  this is shown in Fig. 6. After heating a NaY sample (saturated with  $\text{Fe}(\text{CO})_5$ ) at  $150^\circ\text{C}$  for 10 min, a broad band around  $1940\text{ cm}^{-1}$  with a shoulder at  $1860\text{ cm}^{-1}$  is generated, replacing the  $1985$ ,  $1960$  and  $1945\text{ cm}^{-1}$  bands of the original adduct (Fig. 6D).

The original high frequency bands, in particular the  $2044\text{ cm}^{-1}$  vibration, strongly decrease in intensity after prolonged heating at  $150^\circ\text{C}$ , leaving a shoulder at the  $2005\text{ cm}^{-1}$  band and a weak band at  $2070$  (Fig. 6E).

The broad low frequency band changes into a vibration at  $1900\text{ cm}^{-1}$ , which is the last band to survive by further heating to  $200^\circ\text{C}$ . Decomposition is complete after some hours at  $200^\circ\text{C}$ . No bands below  $1800\text{ cm}^{-1}$  are observed during decomposition.

For the  $\text{Fe}(\text{CO})_5/\text{HY}$  adduct the decomposition is given in Fig. 7. Thermal treatment at  $130^\circ\text{C}$  of a saturated HY-adduct first leads to the generation of a new band around  $1880\text{ cm}^{-1}$  (Fig. 7D), whereas after 7 min. a relative decrease of the low frequency bands at  $1960$  and  $1880\text{ cm}^{-1}$  occurs (Fig. 7E). Prolonged heating at this temperature causes rapid decomposition. After 12 min. only three weak vibrations at  $2065$ ,  $2030$  and  $2000\text{ cm}^{-1}$  are left. Decomposition is completed after 45 min. at  $150^\circ\text{C}$ , and at the same time the original OH-bands are restored to about 75 % of their initial intensity (Fig. 3C).

In both zeolites bands below  $1900\text{ cm}^{-1}$  are formed during the early decomposition, providing some evidence for bridged CO (ref. 18). They may be associated with  $\text{Fe}(\text{CO})_x$  species formed during the first phase of thermal decomposition. Bands at  $1760$  and  $1790\text{ cm}^{-1}$ , which seemed to be characteristic for the  $\text{Fe}_3(\text{CO})_{12}/\text{HY}$  adduct (ref. 12), have never been observed in the present case. The following indications exist for the intermediate formation of  $\text{Fe}_3(\text{CO})_{12}$  :

- on the average 3  $\text{Fe}(\text{CO})_5$  are adsorbed per supercage;
- the average stoichiometry after the first reaction step with HY is  $\text{Fe}(\text{CO})_4$ ;
- bands around  $1880\text{ cm}^{-1}$  which is in the region for bridged CO are also observed for  $\text{Fe}_3(\text{CO})_{12}$  in Ar matrix (ref. 19) or in KBr pellets and in solution (ref. 12). The previously observed bands at  $1760/90\text{ cm}^{-1}$  alternatively can be assigned to surface carbonate (ref. 20,21).

With  $\text{Fe}(\text{CO})_5/\text{NaY}$ , the broad band around  $1895\text{ cm}^{-1}$  is the dominant species before reaction is complete.

In general,  $\text{LFe}(\text{CO})_x$  species exhibit a decrease of CO stretching frequency with decreasing x, if L is a set of the corresponding number of electron donor ligands or an inert matrix (ref. 15,22-24). The present IR results for  $\text{Fe}(\text{CO})_5/\text{NaY}$  can be understood in the same way, indicating a low CO coordination

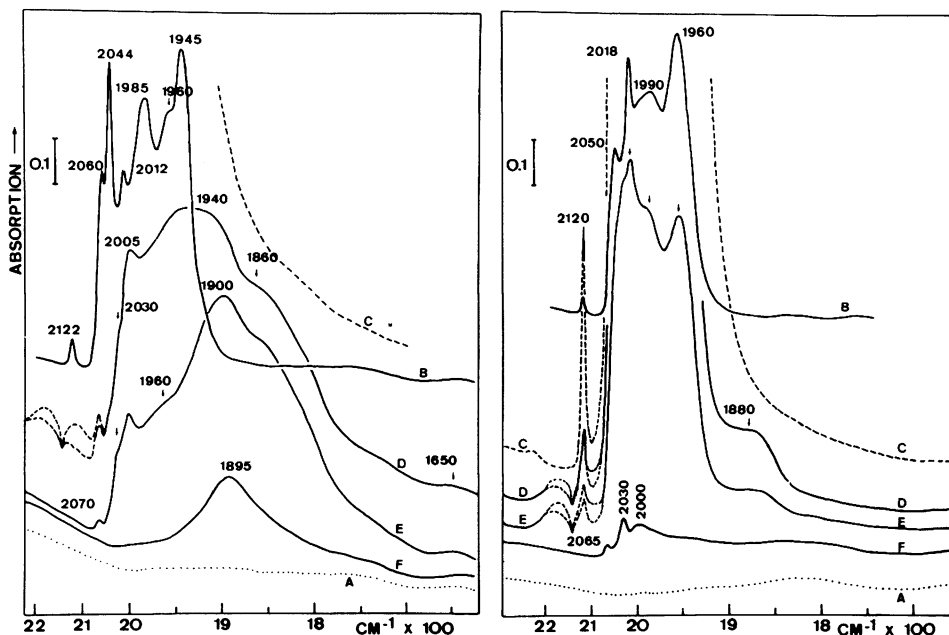


Fig. 6. (left) IR spectra of the decarbonylation of saturated  $\text{Fe}(\text{CO})_5/\text{NaY}$  in He atmosphere.

A : NaY zeolite degassed at  $450^\circ\text{C}$ ; B :  $\text{Fe}(\text{CO})_5/\text{NaY}$  adduct (10 % saturated) at  $20^\circ\text{C}$ ; C :  $\text{Fe}(\text{CO})_5/\text{NaY}$  adduct (saturated) heated in 0.6 bar He at  $100^\circ\text{C}$  for 15 min.; D : sample C heated at  $150^\circ\text{C}$  for 10 min.; E : sample C heated at  $150^\circ\text{C}$  for 30 min., He pumped off; F : sample E heated at  $200^\circ\text{C}$  for 70 min. in 0.6 bar He; A : sample E heated at  $200^\circ\text{C}$  for 5 h.

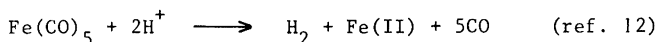
Fig. 7. (right) IR spectra of the decarbonylation of saturated  $\text{Fe}(\text{CO})_5/\text{HY}$  in He atmosphere.

A : HY zeolite degassed at  $450^\circ\text{C}$ ; B :  $\text{Fe}(\text{CO})_5/\text{HY}$  adduct (7 % saturated) at  $20^\circ\text{C}$ ; C :  $\text{Fe}(\text{CO})_5/\text{HY}$  adduct (saturated) at  $20^\circ\text{C}$ ; D : sample C heated up to  $130^\circ\text{C}$  in 0.6 bar He; E : sample D heated at  $130^\circ\text{C}$  for 7 min.; F : sample D heated at  $130^\circ\text{C}$  for 12 min., He pumped off; A : sample D heated at  $150^\circ\text{C}$  for 45 min. in 0.6 bar He.

number of the last generated intermediates.

The lower thermal stability of the HY adduct is explained by weaker  $\pi$ -back-bonding towards the CO ligands due to the increased electron deficiency of the iron clusters. The effect of acidity on the metal-CO bond was also observed with PdHY zeolites (ref. 25).

The HY-hydroxyl groups of the adduct are only partially restored after decomposition, indicating the consumption of protons according to



The portion of oxidized iron, taking into account an initial proton content of  $50 \text{ H}^+/\text{U.C.}$ , may therefore be estimated to be ca. 25 % of the iron loading.

#### CONCLUSION

The present work shows that the iron carbonyl at  $20^\circ\text{C}$  is strongly adsorbed until the supercages of the zeolites are saturated with three molecules on the average. The  $\text{Fe}(\text{CO})_5$  molecule remains intact on adsorption and is encaged in the zeolite with restricted mobility.

In HY, a hydrogen bond of moderate strength is formed with the supercage hydroxyls, which are completely involved in this process. Thermal decomposition in helium of the adducts leads to distinct CO-Fe fragments of different composition. Finally a reproducible iron loading of  $10.5 \pm 0.5 \text{ wt } \%$  is obtained. New evidence is found for the intermediate generation of  $\text{Fe}_3(\text{CO})_{12}$  during the decomposition in HY.

From the partly reversible hydroxyl interaction with the complex in HY, it is estimated that about one quart of the iron is oxidized during decomposition. Thermal decomposition is a slow reaction which goes to completion already between  $70$  and  $90^\circ\text{C}$ . It proceeds faster in case of HY due to acidic destabilization of the Fe-CO bond.

Work is in progress to determine the parameters influencing the particle size and catalytic properties of these zeolite supported iron clusters.

#### ACKNOWLEDGEMENTS

The technical assistance of Hugo Leeman is highly appreciated. One of us (T.B.) is indebted to the DAAD (Deutscher Akademischer Austauschdienst) and the belgian "Ministerie van Nationale Opvoeding en Nederlandse Cultuur" for a grant. P.A.J. acknowledges permanent research position as "Onderzoeksleider" from the Belgian Science Foundation (N.F.W.O.-F.N.R.S.). Financial support from the same institution and from the belgian government (Geconcerteerde Actie Catalyse, Diensten Wetenschapsbeleid) is gratefully acknowledged.

#### REFERENCES

- 1 Kh.M. Minachev, Y.I. Isakov in "Zeolite Chemistry and Catalysis" (J.A. Rabo, ed.) A.C.S., Washington D.C., 1976, p. 552.
- 2 P.A. Jacobs, "Carboniogenic Activity of Zeolites", Elsevier, Amsterdam, 1977.
- 3 Y.-Y. Huang and J.R. Anderson, J. Catal., 40 (1975) 143.
- 4 R.L. Garten, W.N. Delgass and M.J. Boudart, J. Catal., 18 (1970) 90.
- 5 F. Schmidt, W. Gunsser and A. Knappwost, Z. Nat. Forsch., 30a (1975) 1627.
- 6 F. Schmidt, W. Gunsser and J. Adolph, A.C.S. Symp. Ser., 40 (1977) 291.
- 7 W. Gunsser, J. Adolph and F. Schmidt, J. Magn. Magn. Mater., (1980) 1115.
- 8 J.B. Lee, J. Catal., 68 (1980) 27.
- 9 A. Terenin and L.M. Roev, Spectrochim. Acta, 15 (1959) 946.
- 10 J.B. Nagy, M. Van Eenoo and E.G. Derouane, J. Catal., 58 (1979) 230.

- 11 D. Ballivet-Tkatchenko, G. Coudurier, H. Mozzanega and I. Tkatchenko in *Fundament. Res. Homog. Catal.* (Tsutsui ed.) New York, 1979, p. 257.
- 12 D. Ballivet-Tkatchenko and G. Coudurier, *Inorg. Chem.*, 18 (1979) 558.
- 13 M.M. Dubinin, in *Progr. Surf. Membr. Sci.*, D.A. Cadenhead et al., ed., vol. 9 (1975) 1-69.
- 14 R. Cataliotti, A. Foffani and L. Marchetti, *Inorg. Chem.*, 10 (1971) 1594.
- 15 M. Bigorgne, *J. Organomet. Chem.*, 24 (1970) 211.
- 16 W.F. Edgell, W.E. Wilson and R. Summitt, *Spectrochimica Acta*, 19 (1963) 863.
- 17 S. Tanaka, *Bull. Chem. Soc. Japan*, 38 (1965) 795.
- 18 L.H. Little, "Infrared Spectra of Adsorbed Species", A.P., London, 1966, pp. 51.
- 19 M. Poliakoff and J.J. Turner, *J.C.S. Chem. Comm.*, (1970) 1008.
- 20 P.A. Jacobs, F.H. Van Cauwelaert, E.F. Vansant and J.B. Uytterhoeven, *J.C.S. Faraday I*, 69 (1973) 1056.
- 21 P.A. Jacobs, F.H. Van Cauwelaert and E.F. Vansant, *J.C.S. Faraday I*, 69 (1973) 2130.
- 22 B.F.G. Johnson, J. Lewis and M.V. Twigg, *J.C.S. Dalton*, (1974) 241.
- 23 M. Poliakoff and J.J. Turner, *J.C.S. Dalton*, (1974) 2276.
- 24 M. Poliakoff, *J.C.S. Dalton*, (1974) 210.
- 25 P. Gallezot, *Catal. Rev.-Sci. Eng.*, 20(1) (1979) 121.